Accepted Manuscript

Water disinfection by hydrodynamic cavitation in a rotor-stator device

Luis M. Cerecedo, Cesar Dopazo, Rafael Gomez-Lus

PII: S1350-4177(18)30156-1
DOI: https://doi.org/10.1016/j.ultsonch.2018.05.015
Reference: ULTSON 4173

To appear in: *Ultrasonics Sonochemistry*

Received Date: 1 February 2018
Revised Date: 4 May 2018
Accepted Date: 16 May 2018

Please cite this article as: L.M. Cerecedo, C. Dopazo, R. Gomez-Lus, Water disinfection by hydrodynamic cavitation in a rotor-stator device, *Ultrasonics Sonochemistry* (2018), doi: https://doi.org/10.1016/j.ultsonch.2018.05.015

Water disinfection by hydrodynamic cavitation in a rotor-stator device

Luis M. Cerecedo[1,*], Cesar Dopazo[1], and Rafael Gomez-Lus[2]

1 Fluid Mechanics Group, LIFTEC-CSIC-University of Zaragoza, Spain

2 Department of Microbiology, Faculty of Medicine, University of Zaragoza, Spain

*Corresponding author, Tel. +34-976-2672. E-mail address: cerecedo@unizar.es

Abstract

The efficiency of a rotor-stator device for water disinfection based on hydrodynamic cavitation is investigated. Water is infected with *E.coli* and *E.faecalis* with initial concentrations in the range $5\text{x}10^2 - 1.2\text{x}10^6$ CFU/ml. Various geometries of the cavitation channel between rotor and stator are tested, achieving bacterial annihilation in less than 10 minutes of treatment times. Microorganism permanent elimination is verified via micro-seeding to discard viable non-culturable bacteria; micro-seeding was done for those samples displaying no CFU growth via normalized cultures on a Petri dish. TEM photographs are analyzed and the extent of bacterial damages is tentatively correlated with the various cavitation mechanisms. Rotor-stator cavitation assemblies used in the current research are between one and two orders of magnitude more energy efficient than those tested by other investigators. Acoustic pressure spectra are measured to assess the implosion intensity. Parametric analyses are conducted changing the rotor diameter (110-155 mm), the cavitation channel contraction ratio, A_{max}/A_{min} $(4.56 - 5.0)$, and the number of contractions (N_r: $58 - 80$ rotor vanes; N_s: $8 - 16$ stator vanes).

Keywords: Hydrodynamic Cavitation, Water Disinfection, *E.coli*, *E.faecalis*

1. Introduction

The consumption of water infected with various types of microorganisms is an important cause of death in developing countries [1, 2]. The use of chlorine to disinfect water for human consumption has brought about significant benefits. However, some microorganisms are resistant to chlorination [3] and even to temperature [4,5]. Moreover, chlorine can react with the organic matter in the treated water and produce halogenated compounds [6], severely harmful to humans.

Treatment techniques, which avoid using chemicals, such as chlorine, monochloramine or ozone, are of an utmost interest. Advanced photochemical oxidation processes [7] use either solar [8,9] or UV [10] radiations to produce hydroxyl radicals, OH^*, a highly oxidizing agent. Another physically-based technique to induce the generation of OH^* radicals is cavitation [11,12]. Cavitation encompasses the formation, growth and violent collapse of vapor bubbles in a liquid. Low/high liquid pressure variations can be induced via ultrasonic cavitation (UC) [12,13] or hydrodynamic cavitation (HC) [11,14]. Rayleigh [15] showed theoretically that the collapse of an individual bubble entails local temperatures of thousands of °C and pressures of hundreds or thousands of bar, values experimentally and numerically verified [16,17]. The inactivation or total annihilation of *E.coli* with cavitation (UC and HC) [11,18-29] and the oxidation of waterborne chemicals [30, 31] are hence possible.

Stumbling blocks to the use of cavitation as a disinfection method are the unsatisfactory understanding of its basic physical mechanisms and the difficulty to control it, particularly

HC. The small characteristic sizes/times (from a few to some hundreds of microns/microseconds) of bubbles make its observation and measurement extremely difficult. Single bubbles have been extensively investigated and numerically simulated [17,31]. Bubbles appear in practice as clusters, whose measurement and computation also gives rise to serious problems [32-34].

A brief description of the concurrent physical processes in cavitation seems appropriate to facilitate the discussion of the present work [35]. A pressure reduction causes cavitation nuclei (e.g., minute portions of vapor and/or gas trapped in crevices of walls, dirt or suspended particles) to emerge to form bubbles; initial bubble size distributions are determined by the nature of the cavitation nuclei. Should these cavities encounter a low (high) pressure region, they will grow (get smaller); evaporation and condensation take place at the bubble interfaces. A significant increment of pressure can make bubbles with low gas content to collapse violently [15]; cavities become “hot spots”, which can dissociate water vapor within them and produce OH^* radicals, while the interface velocity can reach values of the order of 100 m/s. Experiments and numerical simulations show that bubbles collapsing near walls or in the neighborhood of another cavities adopt non-spherical shapes, which cause the ejection of high speed micro-jets with diameters of a few microns [36]; generated strain rates and shear stresses can be extremely high. Water surrounding a bubble moves inward at a very high speed and it is abruptly stopped near the collapse, generating propagating pressure waves in the liquid. Pressure waves from various cavities in bubble clusters can combine to produce complicated patterns of

intense shock waves [37]. Acoustic and light (sonoluminescence) emissions depend on the bubble implosion intensity. Acoustic micro-streaming can occur in UC [35].

This research examines the efficiency of a rotor-stator assembly to induce intense hydrodynamic cavitation capable of annihilating waterborne CFUs of *E.coli* and *E.faecalis* in small treatment times. The specific objectives of this work are to:

- show that intense hydrodynamic cavitation generated in a rotor-stator device is an efficient and viable water disinfection technique,
- demonstrate that high values of CFU/ml of *E.coli* and *E.faecalis* can be permanently destroyed in short treatment times,
- conduct a preliminary parametric analysis of the cavitation device,
- hypothesize plausible causes of the observed damage to the microorganisms,
- characterize the cavitation intensity under different operating conditions.

Section 2 describes the device used in this work and the microbiological test methodology. Results are presented and discussed in Section 3. Section 4 summarizes the main conclusions and specifies future work.

2. Experimental tests

2.1. Rotor-stator cavitation device

Figure 1 depicts the cavitation assembly used in this research. A rotor moves inside a concentric stator, both equipped with a variable number of vanes on their outer and inner surfaces. The rotor angular velocity can be varied in the range 0-3000 rpm with a 650 W electric motor, current controlled by a potentiometer. A tachometer (Testo-Mod. 470)

was used to measure rpm. The water to be treated fills the channel between rotor and stator and is set in motion by the rotor, flowing across successive contractions and expansions. The water flow is analogous to that through a linear duct with multiple Venturi constrictions in series, but the number of cavitation events experienced by a fluid particle in the rotating arrangement will be much greater than those taking place in a duct with either one or a limited number of contractions. The number of constrictions and expansions can be varied by independently changing the number of rotor, N_r, and stator, N_s, vanes, which, combined with the rotation speed, allows modifying the frequency of cavitation events experienced by a given fluid particle.

Figure 1. Sketch of the rotor-stator cavitation assembly. The number of vanes of both rotor and stator (N_r, N_s) can be varied. Motor/cavitation-device setup.

As a first approximation, the Bernoulli and continuity equations allow estimating the minimum fluid tangential velocity, v_θ, required to reach the liquid vapor pressure, p_v, at the contraction as

$$v_\theta = \left[\frac{h_1+h_2}{R_2-R_1}\left(2-\frac{h_1+h_2}{R_2-R_1}\right)\right]^{-\frac{1}{2}}\sqrt{\frac{2(p-p_v)}{\rho}} \quad (1)$$

R_1 and R_2 are the outer and inner radii of the rotor and stator, respectively, h_1 and h_2 are the radial height of rotor and stator vanes, p is the pressure at the maximum channel width, $R_1 - R_2$, and ρ is the liquid density. Assuming that p equals the atmospheric pressure, v_θ is in the range of 14 to 15 m/s.

The rotor diameter is determined taking into account the minimum tangential velocity and the motor angular velocity ($v_\theta = \Omega R$). Since the main role of the rotor is dragging the water and set it in motion in the rotor-stator channel, a large number of vanes of heights h_1 = 5 mm was used.

The ratio of maximum and minimum channel cross-sectional areas,

$$A_{max}/A_{min} = (R_2 - R_1)/(R_2 - R_1 - h_1 - h_2) \quad (2)$$

is another design parameter to vary in the present study. Note that $R_2 - R_1 - (h_1 + h_2)$ is the rotor-stator minimum gap.

Some initial exploratory MUG tests (to confirm presence or absence of *E.coli*) and analyses of acoustic pressure spectra indicated that 8 and 16 stator vanes produced the best results. However, it is worth noting that many other geometries and operating conditions (e.g., rotor diameter and number of vanes, height of stator vanes, motor rotation speed and power output, gap, …) have been examined in this work. Table 1 summarizes the characteristics of the most efficient prototypes.

Prototype (N_r, N_s)	**R_{rotor} (h_1) (mm)**	**R_{stator} (h_2Xl_2) (mm)**	A_{max}/A_{min} **Gap (mm)**	**Tangential velocity(m/s) (Angular velocity) (rpm)**
Dev.1 (58,8)	55 (5)	92.5 (25X10) (laminated stainless steel)	*5.0* (7.5)	18.85 (3000)

Dev.2 (58,8)	55 (5)	75.5 (11X10) (PVC-160)	*4.56* (4.5)	18.85 (3000)
Dev.3 (80,16)	77.5 (5)	96.5 (10X10) (PVC-200)	*4.75* (4.0)	20.7 (2400)

Table 1. Dimensions and characteristics of three prototypes used in this research.

2.2 Description of microbiological methodology

Two microorganisms have been used in this research to evaluate the disinfection potential of the cavitation device introduced in the previous section: *i*) *E.coli*, a Gram-negative bacterium, used as a worldwide reference to study infected waters [3-5,11,25,30]; *ii*) *E.faecalis*, a Gram-positive fecal coliform bacterium, which inhabits the gastrointestinal tracts of humans and mammals and is resistant to commonly used antibacterial biocides [3]. Both strains belong to the American Type Culture Collection (ATCC): a Gram-negative bacterium, *E.coli* ATCC 25922, and a Gram-positive bacterium, *E.faecalis* ATCC 29212. Strains were grown in agar media at 36 ℃ the night before every test was conducted. The concentration of microorganisms ranged from 10^2 to 10^6 CFU/ml at different stages of the study. Inocula were injected in 5 ml of physiological serum and desired concentrations were determined with a McFarland nephelometer (Dinko Instruments, with a resolution of 0.01 McFarland). Subsequently, the inoculum was diluted in distilled water and this dilution was then injected into the cavitation device; the rotor was then set in motion at 300 rpm (tangential velocity in the range 1.0-2.5 m/s) during 2 minutes to guarantee a

spatially uniform bacterial concentration, which were considered the initial reference samples ($t = 0$). Batch-wise processed volume samples were of 500 ml for Dev.1 and 250 ml for Dev.2 and Dev.3.

Initially, infected water was treated during 10 minutes, withdrawing samples every minute and measuring their temperature. Given the difficulty to eliminate *E.faecalis*, samples were withdrawn after 8, 12, 16 and 20 minutes of treatment. Plate Count Agar (PCA) was used to grow all samples, including the initial reference ones, which were incubated at 36 ℃ for 24 hours. Test results were obtained using the normalized Plate Count Method on Petri dish.

Cell Profiler V.2.0 (a free, open-source, public domain software) was adapted and calibrated to measure very high concentrations ($> 10^3$ CFU/ml) of *E.coli* and for all tests with *E.faecalis*, whose colony-forming units (CFU) display very small sizes (Figure 2) [29].

Figure 2. Differences in sizes of CFU of: a) *E.faecalis* and b) *E.coli*.

2.3 Micro-seeding

Bacterial micro-seeding was performed to determine whether cavitation was capable of either totally eliminating *E.coli* and *E.faecalis* or solely inactivating them. The existence of VBNC bacteria was scrutinized on those Petri dishes observed completely clean by the end of the treatment with prototype Dev.3 (8 and 16 minutes of processing for *E.coli*, and 10 and 30 minutes for *E.faecalis*). The micro-seeding was performed placing a microscope slide over the agar of the Petri dish, which had shown no bacterial growth after 24 hours at 36 ℃ in the oven. Should there be viable microorganisms, they would adhere to the

microscope slide and the Gram staining would make them visible. The various microscope slides used in the micro-seedings were incubated during 4, 7 and 20 hours before Gram staining them.

2.4 Transmission electron microscopy (TEM)

TEM photographs were obtained for a more detailed examination of the potential effects on the microorganism inactivation and destruction of the various cavitation mechanisms used. After the water treatment with Dev.3 for 4, 6, y 8 minutes, 10 ml samples were drawn and centrifuged at 13,000 rpm during 20 minutes. The solid residue was then observed using the transmission electron microscope JEOL JEM-1010, Tokio (Japan) with an acceleration voltage of 100 kV.

3. Results and discussion

3.1 Temperature control

Temperature was measured for every sample withdrawal with a digital thermometer (± 1℃) to control thermal effects, which could contribute to the microorganism elimination. Figure 3 depicts the time evolution of the temperature for the various tests. Temperature temporal increments for cavitation devices Dev.1 and Dev.2 are similar, as they share the same rotor with slightly different stators (Table 1). The fluid temperature increment is a consequence of the viscous dissipation of kinetic energy into heat, which is proportional to the square of the local velocity gradients integrated over the total volume and increases with the geometric tortuosity of the channel between rotor and stator.

Dev.3 displays higher temperatures than Dev.1 and Dev.2 due to the greater number of rotor and stator vanes and to the larger flow velocities and velocity gradients.

Although tests to annihilate *E.faecalis* run for 20 minutes, it was shown that this objective was achieved after 8 minutes of treatment. The final temperatures at the completion of the various treatments never exceeded $58\,℃$ assuring no thermal damage to the microorganisms. Russell and Harries [4] report that the number of CFU/ml increases up to 20% as the temperature rises to $60\,℃$; further temperature increments causes a small decline of CFU/ml (not greater than 10%).

Figure 3. Temperature time evolution in the various cavitation devices used in this research. Numbers (N_r, N_s) in front of (Dev.α; α=1, 2, 3) stand for the number of rotor and stator vanes.

3.2 Bacterial elimination with the various cavitation devices

Figure 4 shows the CFU/ml of *E.coli*, normalized with its initial value, as a function of the treatment time with the three cavitation devices used in this research. Results with Dev.1 display an elimination exceeding 60% after 2 minutes of treatment, followed by a sharp rise to 25% above the initial value at 3 minutes and a slow monotonic reduction thereafter, reaching annihilation at 15 minutes. *E.coli* colonies tend to disaggregate under high mechanical stresses [11,14,21]; after disaggregation, *E.coli* is more vulnerable to cavitation mechanisms, such as, for example, the high shear stresses due to micro-jets, apart from the small-scale turbulent strain rates within the rotor-stator channel. These facts explain the minimum and maximum values of CFU/ml seen in Figure 4.

Figure 4. *E.coli* elimination times with various cavitation devices. CFU/ml are normalized with its initial value, referenced in parenthesis in the legend after Dev.α for α=1, 2, 3. $v_\theta = 18.85\ m/s$ for Dev.1 and Dev.2 and $v_\theta = 20.7\ m/s$ for Dev.3.

Dev.2 exhibits a maximum (less pronounced than that for Dev.1), explainable by the bacterial disaggregation previously mentioned, after 2 minutes of treatment. The efficiency of Dev.2, measured by the treatment time required to eliminate the microorganisms, is greater than that of Dev.1. Differences in the cavitation chamber geometries of Dev.1 and Dve.2 are apparent. The contraction ratio of Dev.2 is almost 10% smaller than that of Dev.1 (see Table.1), which implies a smaller pressure drop in the former (with a less intense cavitation); however, a smaller gap (4.5 mm for Dev.2 compared with 7.5 for Dev.1) leads to a rapid colony disaggregation, due high shear stresses in the constriction, followed by a high probability to act on individual cells. Dev.3 shows a monotonic reduction of CFU/ml for very high initial concentrations in very short treatment times, due to its higher tangential velocity, its smaller gap and its greater number of contractions/expansions.

Process times of *E.faecalis* elimination tests with Dev.1 and Dev.2 increased moderately, which suggested the convenience of trying Dev.3 with more intense cavitation features. The design of the Dev.3 prototype aimed at achieving more intense and frequent bubble implosions. First, a greater rotor diameter allows increasing the tangential velocity and decreasing the minimum pressure at the rotor-stator throat (minimum gap). Whereas a 37% increment of the rotor diameter leads to an equal boost of the flow mean velocity,

also implies multiplying the required power by a factor of 4.83. Second, the stator diameter must also be increased; a ratio ($A_{máx}/A_{mín}$) of 4.75 was decided, similar to that of Dev.2 (4.56). Third, changing the number of stator vanes from 8 to 16 doubles the number of cavitation events a portion of fluid experiences.

Figure 5 presents a comparison of the effectiveness of Dev.3 to treat *E.coli* and *E.faecalis*. Results are not normalized. Results for the treatment of *E.coli* with Dev.2 are also plotted as a reference.

Figure 5. Elimination efficiency of Dev.3 for infected water with *E.coli* (Gram-negative) and *E.faecalis* (Gram-positive). Results for Dev.2 with *E.coli* are also included.

An increment of the number of channel contractions and divergent sections increases the number of cavitation events a fluid particle undergoes. However, it was decided to limit the number of rotor and stator vanes to possibly avoid what is termed *choked cavitation* [31], which produces bubble coalescence and reduces the implosion intensity and the treatment success [43].

3.3 Micro-seeding: Viable but nonculturable (VBNC) microorganisms

Figure 6 show results of Gram staining for the case of *E.coli*. Figure 6.a displays a photograph of a sample withdrawn after 4 minutes of treatment, in which it was possible to observe and count the CFU. This sample was of help to prove the correctness of the staining technique; a rod-shape is characteristic of *E.coli*. On the other hand, Figure 6.b depicts a microscope photograph of a micro-seeding from a clean Petri dish with no visible bacterial presence, with only remains of the Gram stain observed; had rod-shape bacteria

been present in the treated sample, existing VBNC microorganisms could perhaps become active and reproduce to create CFU. The absence of VBNC microorganisms in Figure 6.b guarantees that the treatment process not only inactivates bacteria but it is also capable of annihilating them.

Figure 6. Gram staining of two micro-seedings of *E.coli* incubated for 20 hours. a) micro-seeding of a sample after 4 minutes of treatment; b) micro-seeding of a sample after 16 minutes of treatment.

3.4 Possible cavitation mechanisms responsible for bacterial annihilation

Transmission electron microscopy (TEM) allows formulating some preliminary conjectures or interpretations of the effects of various cavitation mechanisms that might contribute to the bacterial elimination. Figure 7 presents photographs of *E.coli* cells at different treatment times. At an early stage in the process (Figure 7.b), morphological changes of the microorganism are apparent in the form of either coagulation of cytoplasmic matter (**1**) or absence of matter in the periplasmic space (**2**). As the treatment time increases (Figure 7.c and 7.d), generalized membrane ruptures (**3**) occur in addition to (**1**) and (**2**); the absence of cytoplasmic and periplasmic matter, due to the release of intracellular components, is also noticeable.

Figure 7. TEM photographs of *E.coli* cells. a) Untreated bacteria; b), c) and d) after 4, 6 and 8 minutes of treatment. **1**) Coagulation of cytoplasmic matter; **2**) Absence of cytoplasmic matter; **3**) Membrane rupture.

The various physical processes and mechanisms of cavitation have been qualitatively or semi-quantitatively described in the Introduction. It is only possible to conjecture about plausible causes of the observed cellular damages. For example, the coagulation of cytoplasmic matter could be attributed to strong shock waves propagating in the liquid; similar effects have been observed when *E.coli* is subject to high hydrostatic pressures [5]. On the other hand, high temperatures at bubble implosions (hot spots) could be responsible for the absence of matter in the periplasmic space. Although membrane ruptures could be likely caused by extremely high shear stresses of micro-jets [24], the contributions of OH^* radicals, high temperatures and shock waves cannot be discarded. The individual and joint effects of the various cavitation mechanisms need further and detailed investigation.

3.5 Energy efficiency estimates

It is possible to estimate the energy efficiency of the various experimental devices reported in this work from results in Figures 4 and 5 and the technical characteristics of the equipment. Firstly, the CFU eliminated per unit of energy (CFU_{killed}/J) used in the process is readily calculated and compared with those for other treatments [11,14,28]; the work of Gao et al. [28], which treats *Enterobacter aerogenes* (gam-negative) with low-frequency (20 kHz) ultrasounds, is selected for the excellent reported results. Secondly, the energy required to reduce 90% or, equivalently, one order of magnitude (from 100% to 10%, which implies $\log(\mathrm{CFU}_{\mathrm{initial}}/\mathrm{CFU}_{\mathrm{final}}) = 1.0$) the initial CFU was also computed, according to the relationship

$$E\left(\frac{kWh}{l}\right) = \frac{\dot{W}(kWh)}{V_{sample}(l)} \cdot \frac{t_{treat}(hr)}{log\left(CFU_{ini}/CFU_{final}\right)} \quad (3)$$

For example, in the case of Dev.3 with *E.coli*, the electric motor power is $650\,W = 0.65\,kW$, the processed sample volume $250\,ml = 0.25\,l$ and the treatment time is $8\,min = 8/60\,hr$. From the results in Figure 4, $CFU_{ini} = 5.8x105\,CFU/ml$ y $CFU_{final} = 0\,CFU/ml$; to avoid an indeterminacy it is taken CFU_{final} = 1 CFU/ml. Hence,

$$E\left(\frac{kWh}{l}\right) = \frac{0.65\,(kW)}{0.25\,(l)} \frac{8/60\,(hr)}{log\left(\frac{5.8 \cdot 10^5}{1}\right)} = 0.06\left(\frac{kWh}{l}\right)$$

Table 2 depicts these energy efficiency indicators for the devices and operating conditions used in this research and compares them with those of various processes and equipments utilized by other investigators [11,14,28]. The current hydrodynamic cavitation devices are apparently capable of totally eliminating higher initial bacterial concentrations with lower energy consumption in significantly smaller times than alternative processes and equipments [11,14,28], with no additional use of chemicals. It is worth noting that Reference [14] dealt with disinfection of bore well water for potable use; therefore, a comparison with results of this manuscript is not straightforward. However, with this caveat, the devices used in the current research seem much more energy efficient than ultrasonic and hydrodynamic (orifice plate) cavitations. Only the high speed homogeneizer [14], which is apparently based on the same concept, seems comparable with Dev.2 and Dev.3 in energy terms, although with longer treatment times.

Device	Sample volume	Treatment time (hr)	Electric energy	CFU killed/ml	Disinfection based on electrical energy	$E\left[\frac{kWh}{l}\right]$ (Eq.3)

	[ml]		consumption kWh		consumption $(CFU\ killed/J)$	
Dev.1	500	0.25	0.65	5.0×10^2	0.43	0.12
Dev.2	250	0.10	0.65	3.2×10^4	34.19	0.06
Dev.3 (*E.coli*)	250	0.13	0.65	5.8×10^5	480.77	0.06
Dev.3 (*E.faecalis*)	250	0.17	0.65	1.2×10^6	769.23	0.07
HC orifice plate (*E.coli*) [11]	50 000	2.0	5.0	9×10^3	12.5	1.49
HC Venturi V6 (*E.coli*) [11]	50 000	2.0	5.0	4.3×10^4	59.88	0.145
Ultrasonic homogenizer (E.aerogenes) [28]	15	1.0	0.008	1.19×10^8	62,496.79	0.124
Ultrasonic horn (bore well water) [14]	50	0.25	0.240	5.7×10^3	1.33	1.61
High speed homogeneiser (bore well water) [14]	1 000	0.25	0.105	2.2×10^3	23.92	0.02
HC valve at 5.17 bar (bore well water) [14]	75 000	0.25	5.50	9.2×10^2	13.94	0.16

Table 2. Estimated energy efficiency of the various bacterial elimination devices used in this research and a comparison with different processes and devices utilized by other investigators (Jyoti and Pandit, 2001; Arrojo et al., 2008; Gao et al., 2014).

3.6 Cavitation characterization through acoustic pressure spectra

Observation of micro-scale (microns and micro-seconds) fluid dynamic phenomena occurring in cavitation is extremely difficult. However, it is important characterizing its

essential features, for example, to estimate the cavitation intensity directly linked to the bacterial annihilation efficiency. The development of heuristic methods to assess the influence of various operating parameters on the behavior of bubble clusters is pivotal to devise innovative, efficient and controllable disinfection techniques, before a better understanding of the cavitation physics is reached.

The macroscopic characterization of the cavitation intensity can be more easily assessed through acoustic pressure measurements [13,38-40]. Gauged acoustic signals are converted, using a piezoelectric sensor (diameter of $20\ mm$, with a resonance frequency of $6.5\ MHz$ and a maximum output voltage of $12\ V$), to electric signals, which are then conditioned with a Reson, Mod. EC6081 preamplifier, including filtering. The conditioned signal is acquired through a data acquisition card, PCI-MIO-16E-1, from National Instruments. Acoustic signals of the various cavitation devices investigated in this work have been transduced and analyzed with a data acquisition subroutine in LabVIEW [39,40] developed as a part of the current research. Signals have been analyzed in the frequency domain via FFT.

Figure 8 depicts pressure spectra at different maximum flow velocities for prototype Dev.3. Two distinct ranges are apparent for low (< 1 kHz) and high (> 1 kHz) frequencies. The former are associated to vortical macro-structures; it has been observed that the vortex shedding frequency, f_{vort}, from a jet of diameter D and exit velocity U define a Strouhal number, S_H, given by [41],

$$S_H = f_{vort}\frac{D}{U} \approx 0.32 \tag{4}$$

Extrapolation of equation (4) to the cavitation device, with $U = v_\theta$ and $D = (R_2 - h_2) - (R_1 + h_1)$, yields,

$$f_{vort} = 0.32 \frac{v_\theta}{(R_2 - h_2) - (R_1 + h_1)} \quad (5)$$

Table 3 shows results obtained with equation (5). These results approximately coincide with low frequencies observed in the acoustic pressure spectra of Figure 8. Notice that these structures become more intense (higher rms values) as the flow velocity increases. On the other hand, the rms pressure fluctuations at high frequencies are associated with the rotor vane passages, whose frequencies, for a rotor with N_r vanes, are

$$f_{vanes} = \frac{\Omega}{60} N_r \quad (6)$$

Therefore, these frequencies are proportional to the angular speed, Ω.

Figure 8. Acoustic pressure spectra for Div.3 ($N_r = 80, N_s = 16$) at different maximum flow velocities. Peaks observed at high frequencies (> 1 kHz) correspond to passages of rotor vanes (Table 2).

Ω (rpm)	**Maximum v_θ of rotor periphery (m/s)**	**Mean v_θ at contractions (m/s)**	**f_{vort} (Hz)**	**f_{vanes} (Hz)**
1070	9.2	4.62	147.1	1427
1450	12.5	6.25	199.4	1930
2060	17.8	8.9	283.3	2746
3000	25.9	12.95	412.5	4000

Table 3. Characteristic frequencies for Dev.3 as a function of tangential velocity.

The acoustic pressure spectrum at 25.9 m/s shows a mound between 1 kHz and 2 kHz (Figure 8), which is not present at other flow velocities. Frequencies in this range are related to the presence of cavitation bubbles; in fact, this spectrum is typical of the sound emission by cavitation, which is well known in hydraulic turbomachinery [42].

Figure 9 depicts a comparison between acoustic pressure spectra for Dev.3 with different numbers of stator vanes. As the number of vanes or, equivalently, of subsequent contractions, increases the spectral power at low frequencies slightly decreases, whereas that at high frequencies increases, which denotes either a higher number of bubbles or more intense implosions; both effects contribute to bacterial colony disaggregation followed by microorganism damages, and to a reduction of the treatment time (Figure 5).

Figure 9. Acoustic pressure spectra for Dev.3 with different numbers of stator vanes ($v_\theta = 16\ m/s$; $f_{vanes} = 2450\ Hz$): a) $N_s = 8$; b) $N_s = 16$.

4. Conclusions.

The efficiency of a rotor-stator device for water disinfection based on hydrodynamic cavitation has been investigated. Water was infected with *E.coli* and *E.faecalis* with initial concentrations in the range $5\text{x}10^2 - 1.2\text{x}10^6\ CFU/ml$. Different geometries of the cavitation channel between rotor and stator have been successfully tested, achieving bacterial annihilation in small treatment times (≤ 10 minutes). Microorganism total and permanent elimination has been verified via micro-seeding after the completion of the treatment for those samples in which a total absence of microorganisms was observed. TEM photographs have been analyzed and the extent of bacterial damages has been

tentatively correlated with the various cavitation mechanisms. Acoustic pressure spectra have been used to assess the implosion intensity.

Parametric analyses have been conducted changing rotor diameter, R_{rotor}, the channel contraction ratio, A_{max}/A_{min}, the minimum gap and the number of contractions, (N_r, N_s). The following remarks seem pertinent:

1. An increment of the rotor diameter implies both higher mean fluid velocity at the contractions and pressure reductions, which yield higher implosion intensity within the rotor-stator channel. However, bigger rotor dimensions require larger torques and power consumptions.
2. The reduction of the gap between rotor and stator, $(R_2 - R_1) - (h_1 + h_2)$, by 40% (Table 1) brings about significant benefits, such as greater strain rates and higher efficiency in bacterial colony disaggregation.
3. For a larger number of contractions the number of cavitation events experienced by a fluid particle increases. Doubling the number of contractions allowed eliminating the resistant *E.faecalis*.
4. Energy efficiency of the various devices tested in this research has improved along the project development from Dev.1 to Dev.3. This proves that the different variables changed for every test are the relevant ones. It is tentatively concluded that energy consumption of the present rotating device is smaller than that of alternative ultrasonic and hydrodynamic cavitation equipment employed by other investigators.

5. Acoustic pressure spectra confirm some intuitive notions on the correlation between greater bubble concentration and higher spectral power at high frequencies, also connected with intense implosions.

The capacity of this rotating cavitation device to totally eliminate spore-forming bacteria and viruses should be demonstrated as a follow-up of the present research. The addition of small concentrations of specific chemicals (e.g., H_2O_2 or O_3) should be tested to estimate increments in biocidal effects and in the reduction of treatment times. The oxidation of some chemical compounds is also possible with this device. A final target of this research is the design of a cavitation pilot plant for continuous flow operation.

Acknowledgements

Authors would like to acknowledge the use of Servicio General de Apoyo a la Investigación-SAI, University of Zaragoza. The authors would also like to thank J. A. Bueno and L. Abadía for their collaboration during this work.

References

[1] WHO, Media Center (2015), *Drinking-water*, Fact-sheet Nº 391.

[2] WHO and UNICEF (2014), *Progress on Drinking Water and Sanitation*, Update.

[3] Mir, J., Morató, J. and Ribas, F. (1997), *Resistance to chlorine of freshwater bacterial strains*, J. Appl. Microbiology **82**, 7-18.

[4] Russell, A.D. and Harries, D. (1967), *Some Aspects of Thermal Injury in Escherichia coli*, J. Appl. Microbiology **15**, 407-410.

[5] Moussa, M., Perrier-Cornet, J.M. and Gervais, P. (2007), *Damage in Escherichia coli Cells Treated with a Combination of High Hydrostatic Pressure and Subzero Temperature*, Appl. Environ. Microbiology **73**, 6508–6518.

[6] Simpsom, K.L. and Hayes, K.P. (1998), *Drinking water disinfection by-products: an Australian perspective*, Water Res. **32**, 1522-1528.

[7] US-EPA, Handbook (1998), *Advanced Photochemical Oxidation Processes*, Center for Environmental Research Information.

[8] Gelover, S., Gomez, L. A., Reyes, K. and Leal, M. T. (2006), *A practical demonstration of water disinfection using TiO_2 films and sunlight*, Water Res. **40**, 3274-3280.

[9] Rincon, A.G. and Pulgarin, C. (2007), *Absence of E. coli regrowth after Fe^{3+} and TiO_2 solar photoassisted disinfection of water in CPC solar photoreactor*, Catalysis Today **124**, 204-214.

[10] Sun, P., Tyree, C. and Huang, C.H. (2016), *Inactivation of Escherichia coli, Bacteriophage MS2 and Bacillus Spores under UV/H2O2 and UV/Peroxydisulfate Advanced Disinfection Conditions*, Environ. Sci. Technol. **50**, 4448-4458.

[11] Arrojo, S., Benito, Y. and Martinez, A. (2008), *A parametrical study of disinfection with hydrodynamic cavitation,* Ultrason. Sonochem. **15**, 903-908.

[12] Gong, C. (1999), *Ultrasound Induced Cavitation and Sonochemical Effects*, PhD Dissertation, Mass. Inst. Technol.

[13] Avvaru, B. and Pandit, A.B. (2009), *Oscillating bubble concentration and its size distribution using acoustic emission spectra*, Ultrason. Sonochem. **16**, 105-115.

[14] Jyoti, K.K. and Pandit, A.B. (2001), *Water disinfection by acoustic and hydrodynamic cavitation*, Biochem. Engng J. **7**, 201–212.

[15] Rayleigh (Lord) (1917), *Pressure developed in a liquid during the collapse of a spherical cavity,* Phil. Mag. **34**, 94-98.

[16] Flint, E.B. and Suslick, K.S. (1991), *The temperature of cavitation*, Science **253**, 1397-1399.

[17] Hauke, G., Fuster, D. and Dopazo, C. (2007), *Dynamics of a single cavitating and reacting bubble*, Phys. Rev. E **75**, 066310-1 / 0066310-14.

[18] Wood, R.W. and Loomis, A.L. (1927), *Biological effects of ultrasound*, Phil. Mag., Ser. **7**, 4, 417-436.

[19] Johnson, C.H.(1929), *The lethal effects of ultrasonic radiation*, J. Physiol. **67**, 356-359.

[20] Suslick, K.S. (1989), *Ultrasound: Its Chemical, Physical, and Biological Effects*, VCHPublisher, New York.

[21] Joyce, E., Phull, S.S., Lorimer, J.P. and Mason,T.J. (2003), *The development and evaluation of ultrasound for the treatment of bacterial suspension. A study of frequency, power and sonication time on cultured Bacillus species*, Ultrason. Sonochem. **10**, 315-318.

[22] Gogate, P.R. and Kabadi, A.M. (2009), *A review of applications of cavitation in biochemical engineering/biotechnology*, Biochemical Engineering Journal, **44**, 60-72.

[23] Scheie, P. and Ehrenspecke, S. (1973), *Large Surface Blebs on Escherichia coli Heated to Inactivating Temperatures*, J. Bacteriol. **114**, 814-818.

[24] Hewitt, C.J., Boon, L.A., McFarlane, C.M. and Nienow, A.W. (1998), *The Use of Flow Cytometry to Study the Impact of Fluid Mechanical Stresses on Escherichia coli W3110 During Continuous Cultivation in an Agitated Biorreactor*, Biotechnol. Bioeng. 0006-3592/98/050612-09.

[25] Hua, I. and Thompson, J.E. (2000), *Inactivation of Escherichia coli by sonication at ultrasonic frequencies*, Water Res. **34**, 3888-3893.

[26] Furuta, M., Yamaguchi, M., Tsukamoto, T., Yim, B., Stavarache, C.E., Hasiba, K. and Maeda, Y. (2004), *Inactivation of Escherichia coli by ultrasonic irradiation*, Ultrason. Sonochem. **11**, 57-60.

[27] Ananta, E., Voigt, D., Zenker, M., Heinz, V. and Knorr, D. (2005), *Cellular injuries upon exposure of Escherichia coli and Lactobacillus rhamnosus to high-intensity ultrasounds*, J. Appl. Microbiol. **10**, 271-278.

[28] Gao, S., Lewis, G.D., Ashokkumar, M. and Hemar, Y. (2014), *Inactivation of microorganisms by low-frequency high-power ultrasound: 2. A simple model for the inactivation mechanism*, Ultrason. Sonochem. **21**, 454-460.

[29] Dopazo, C., Cerecedo, L.M., and Gomez-Lus, R. (2016), *New water physical treatment based on hydrodynamic cavitation* (in Spanish), Anales de la Real Academia Nacional de Medicina, Spain, 703-714.

[30] Hua, I. and Hoffmann, M.R. (1997), *Optimization of ultrasonic irradiation as an advanced oxidation technology,* Environ. Sci. Technol. **31**, 2237-2243.

[31] Badve, M., Gogate, P., Pandit, A. and Csoka, L. (2013), *Hydrodynamic cavitation as a novel approach for wastewater treatment in wood finishing industry*, Separ. Purif. Technol. **106**, 15–21.

[32] Gaitan, D.F., Crum, L.A., Church, C.C. and Roy, R.A. (1992), *Sonoluminescence and bubble dynamics for a single, stable, cavitation bubble*, J. Acoust. Soc. Am. **91**, 3166-3183.

[33] Franc, J.P. and Michel, J.M. (2004), *Fundamentals of cavitation*, Springer.

[34] Fuster, D. and Colonius, T. (2011), *Modelling bubble clusters in compressible liquids*, J. Fluid Mech. **688**, 352-389.

[35] Egerer, C.P., Hickel, S., Schmidt, S.J. and Adams, N.A. (2014), *Large-eddy simulation of turbulent cavitating flow in a micro channel*, Phys. Fluids **26**, 085102.

[36] Brennen, C.E. (1995), *Cavitation and Bubble Dynamics*, Oxford Univ. Press.

[37] Plesset, M. S. and Chapman, R. B. (1971), *Collapse of an initially spherical vapour cavity in the neighbourhood of a solid boundary*, J. Fluid Mech. **47**, 283–290.

[38] Wang, Y-C. (1996), *Shock Waves in Bubbly Cavitating Flows*, PhD Dissertation, Calif. Inst. Technol.

[39] Abadia, L. (2012), *Experimental study of hydrodynamic cavitation from its acoustic pressure spectra* (in Spanish), Graduation Project, Chemical Engineering, University of Zaragoza.

[40] Abadia, L. (2014), *Experimental study of the hydrodynamics of cavitating flows: Optimization of a hydrodynamic cavitation equipment* (in Spanish), MSc Thesis, Applied Mechanics, University of Zaragoza.

[41] Crow, S.C. and Champagne, F.H. (1971), *Orderly structure in jet turbulence*, J. Fluid Mech. **48**, 547-591.

[42] Birajdar, R. and Khanzode, K. (2009), *Vibration and noise in centrifugal pumps – source and diagnosis methods,* 3rd Int. Confer. Integrity, Reliability and Failure, Porto-Portugal.

[44] Jyoti, K.K. and Pandit, A.B. (2003), *Hybrid cavitation methods for water disinfection: simultaneous use of chemicals with cavitation*, Ultrason. Sonochem. **10**, 255-264.

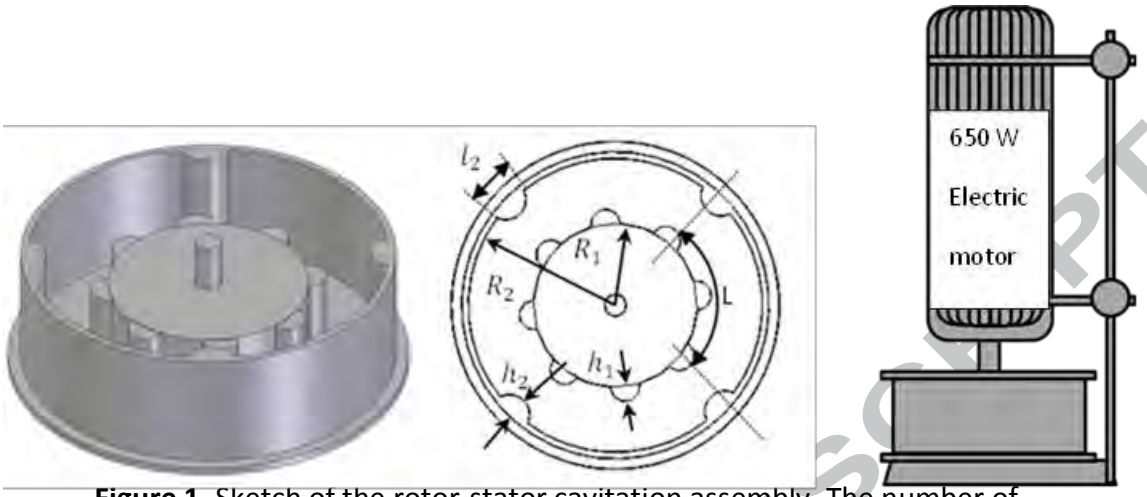

Figure 1. Sketch of the rotor-stator cavitation assembly. The number of vanes of both rotor and stator (N_r, N_s) can be varied. Motor/cavitation-device setup.

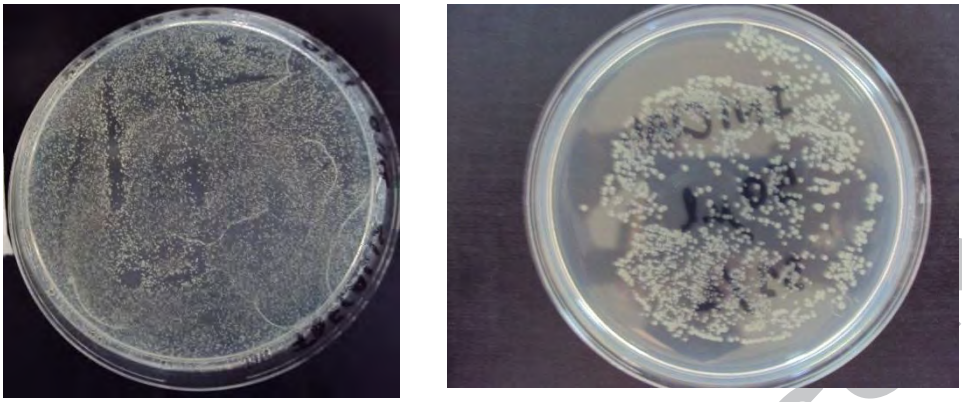

a) b)

Figure 2. Differences in sizes of CFU of: a) *E.faecalis* and b) *E.coli*.

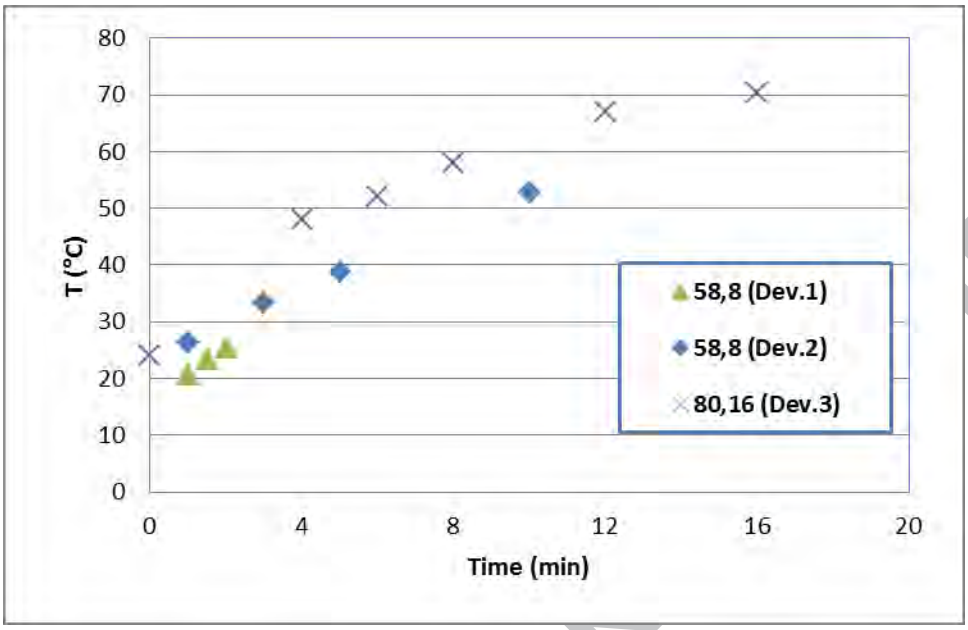

Figure 3. Temperature time evolution in the various cavitation devices used in this research. Numbers (N_r, N_s) in front of (Dev.α; α=1, 2, 3) stand for the number of rotor and stator vanes.

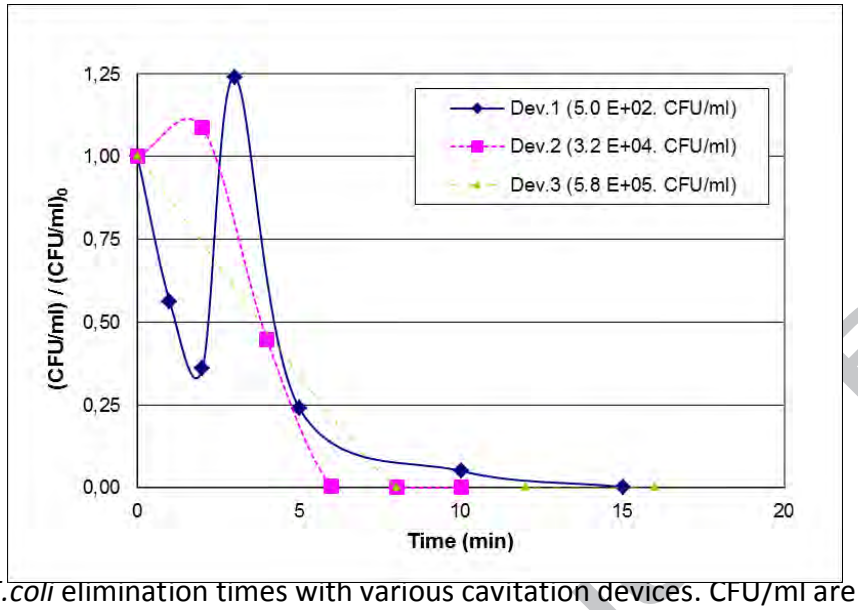

Figure 4. *E.coli* elimination times with various cavitation devices. CFU/ml are normalized with its initial value, referenced in parenthesis in the legend after Dev.α for α=1, 2, 3. $v_\theta = 18.85\ m/s$ for Dev.1 and Dev.2 and $v_\theta = 20.7\ m/s$ for Dev.3.

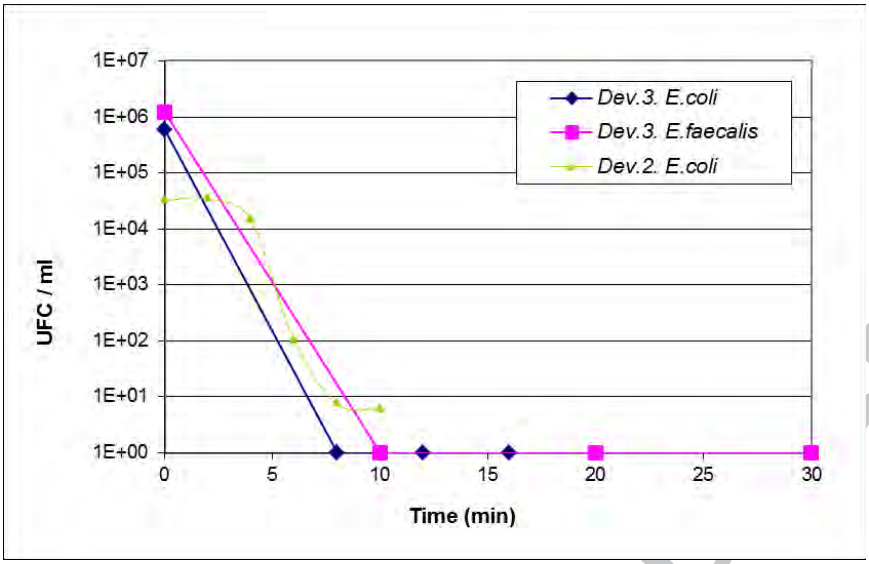

Figure 5. Elimination efficiency of Dev.3 for infected water with *E.coli* (Gram-negative) and *E.faecalis* (Gram-positive). Results for Dev.2 with *E.coli* are also included.

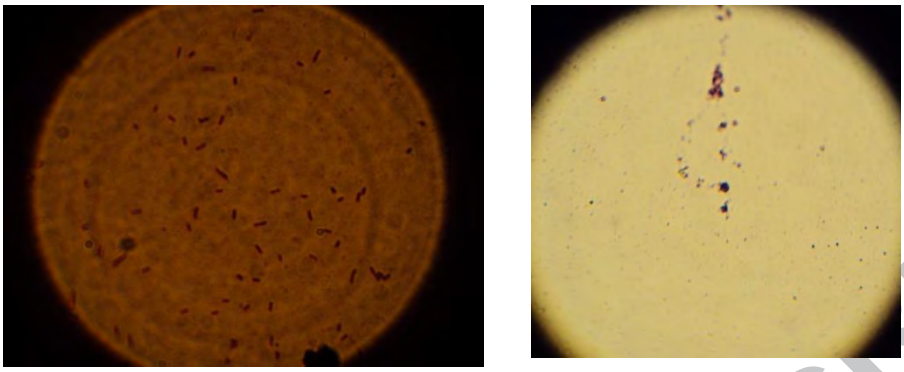

a) b)

Figure 6. Gram staining of two micro-seedings of *E.coli* incubated for 20 hours. a) micro-seeding of a sample after 4 minutes of treatment; b) micro-seeding of a sample after 16 minutes of treatment.

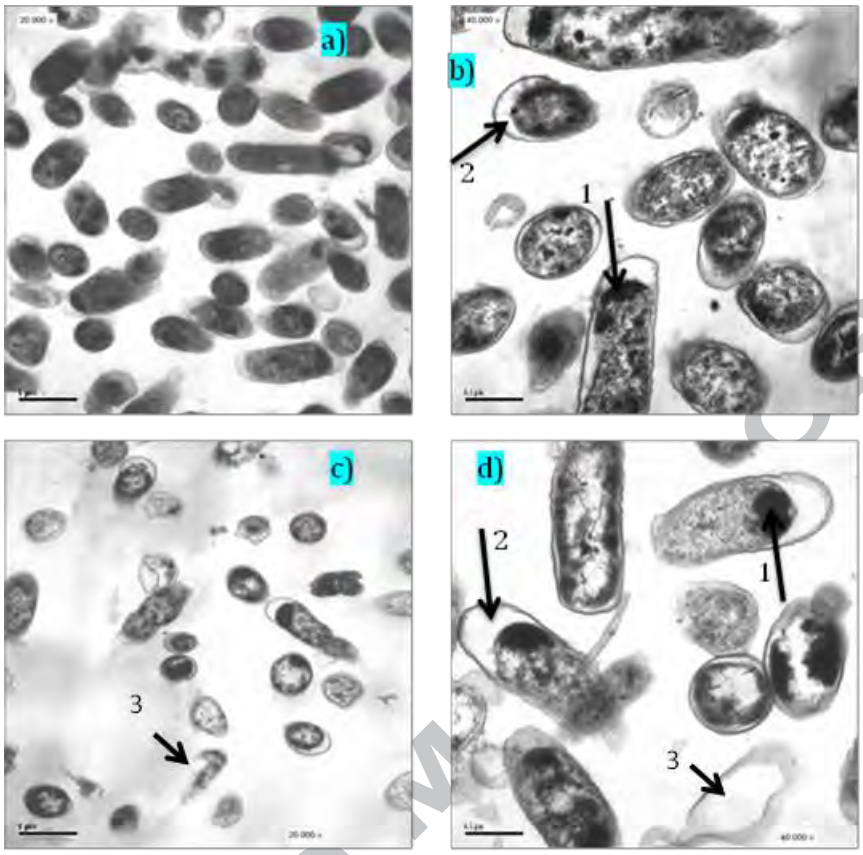

Figure 7. TEM photographs of *E.coli* cells. a) Untreated bacteria; b), c) and d) after 4, 6 and 8 minutes of treatment. **1**) Coagulation of cytoplasmic matter; **2**) Absence of cytoplasmic matter; **3**) Membrane rupture.

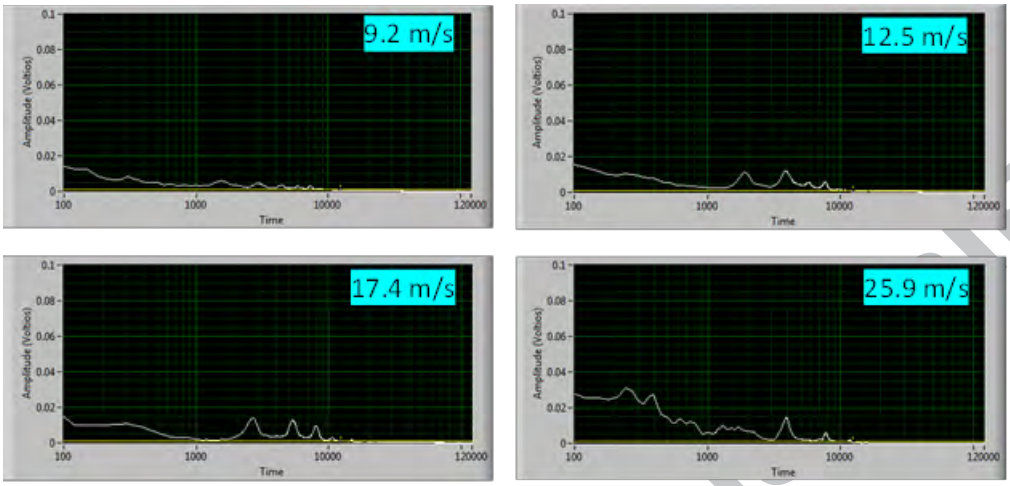

Figure 8. Acoustic pressure spectra for Div.3 ($N_r = 80, N_s = 16$) at different maximum flow velocities. Peaks observed at high frequencies (> 1 kHz) correspond to passages of rotor vanes (Table 2).

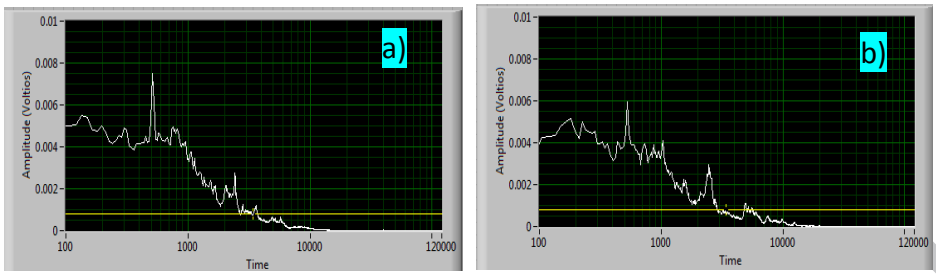

Figure 9. Acoustic pressure spectra for Dev.3 with different numbers of stator vanes ($v_\theta = 16\ m/s$; $f_{vanes} = 2450\ Hz$): a) $N_s = 8$; b) $N_s = 16$.

Highlights

→ An efficient disinfection method based on hydrodynamic cavitation is investigated.

→ A rotor-stator device for water disinfection based on hydrodynamic cavitation is investigated.

→ High concentrations of *E.coli* and *E.faecalis* are annihilated in less than 10 minutes.

→ Energy efficiency is up two orders of magnitude more efficient than other cavitation based devices.

→ Geometries, operating variables and cavitation intensity are changed and characterized.